Z. Phys. C – Particles and Fields 49, 267–275 (1991)

Zeitschrift für Physik C Particles and Fields

Higgs production and background at LEP

K.J.F. Gaemers and N. de Groot

NIKHEF-H, P.O. Box 41882, NL-1009 DB Amsterdam, The Netherlands

Received 18 December 1989; in revised form 13 May 1990

Abstract. We calculate the total cross section for the process $e^+e^- \to \mu^+\mu^- b\bar{b}$ at tree level for LEP energies. We take into account the Higgs production subprocess, background processes with two intermediate vector bosons and their interference. A Higgs lighter than 50 GeV could be observed at LEP 1. In this case the background can easily be eliminated. For a heavier Higgs we need LEP 200 energies. Here we will get a significant background from double Z production.

1 Introduction

One of the interesting possibilities that LEP offers is the search for the Higgs boson. The relevant production mechanism has already been studied extensively in the litterature ([1-4] and the references therein). The basic process can be written as:

$$e^+e^- \to Z + H. \tag{1}$$

Depending on the c.m.s. energy we distinguish two regimes:

a) The c.m.s. energy is so low that the Z has to be off-shell.
b) The c.m.s. energy is high enough so that both the Z and the H are on shell.

We have to keep in mind however that both the Z and the H are instable particles so that the remarks above are true if one neglects finite width effects.

In order to study the process (1) experimentally one must observe the decay products of the Z and the H. Let us first consider the decay of the Higgs. From preliminary studies it is clear that LEP will be able to observe a Higgs if its mass is less than ≈ 80 GeV. Given the current lower limit on the mass of the top quark of 77 GeV, it is not necessary for a Higgs search at LEP to consider the decay:

$$H \to t\bar{t}. \tag{2}$$

From this it must be concluded that if the Higgs has a mass in the range from 10 to 80 GeV the only decay modes that can possibly be observed are:

$$H \to c\bar{c}$$
$$H \to \tau\bar{\tau}$$
$$H \to b\bar{b}. \tag{3}$$

If the Higgs has a mass greater than 15 GeV, as the first analysis of LEP data indicates [5], only the last decay mode of (3) needs to be considered, because then $B(H \to b\bar{b}) > 0.75$.

Next we look at the decay products of the Z. Here the situation is quite different from that of the H. The Z can decay into quark or lepton pairs with braching ratios that do not differ by more than a factor 4 from one another. In order to have a definite experimental signature it is probably the least difficult to study the H decay into $b\bar{b}$ and the Z decay into $\mu^+\mu^-$. In other words we consider:

$$e^+e^- \to \mu^+\mu^- b\bar{b} \tag{4}$$

which in lowest order is described by the Feynman diagram in Fig. 1.

In the context of the standard model there are several other processes leading to the same final state as reaction (4). It is the purpose of this paper to study these background processes in order to assess their relative importance and also study interference effect of the background and Higgs production.

In order to keep the mathematics as simple as possible we consider all processes at the amplitude level and we do not use conventional trace techniques. The formalism that we use has been worked out by Berends, Daverveldt and Kleiss [6]. Here we extend their formalism, which is given for vector and axial vector interactions only, to scalar interactions, which are necessary for the Higgs couplings. The outline of our paper is as follows. In Sect. 2 we review the amplitude formalism of [6] and we give the extension for Higgs couplings. In Sect. 3 we present details of the phase space and Monte Carlo calculations. In Sect. 4 finally, we present numerical results on the background and the interference as well as a discussion of the implications.

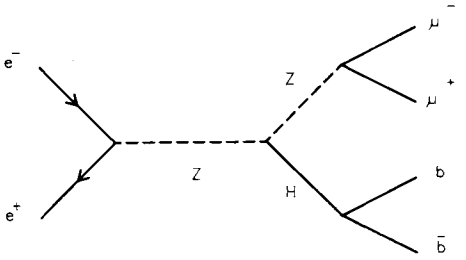

Fig. 1. Feynman diagram for Higgs production

2 Matrix elements

As indicated in the introduction there are several diagrams that contribute to reaction (4). In Fig. 2 we present the subset of these diagrams that we will consider. The remaining diagrams are of final state radiation processes; one of the fermions, created by a Z or a photon radiates another photon or Z that decays into another fermion pair. In this paper we will neglect these diagrams for the following reasons. The basic process of Fig. 1 connects the μ pair to a virtual Z, which leads to a mass spectrum for the μ pairs peaking at high invariant masses. The diagrams of Fig. 2 will mimic this behaviour, whereas the other diagrams will not. Combining the diagrams of Fig. 1 and 2 we see that in this approximation our amplitude gets a contribution from 9 diagrams. It is now clear that using the conventional technique of squaring and taking Dirac traces would be extremely cumbersome. Here we opt for the (pseudo) helicity formalism of [6]. The basic ingredient of this method is a formal 4 fermion amplitude which we will denote, following [6] by $Z(l, l, l, l)$ for completeness we give these amplitudes in the appendix. With these Z functions for general vector and axial couplings we can completely give the amplitudes corresponding to the diagrams in Fig. 2. For the diagram in Fig. 1 however, we must introduce an amplitude corresponding to a scalar coupling as an extra ingredient. The pseudo helicity amplitude technique works as follows: We define spinors $u_\lambda(p)$ which are normalised by

$$\sum_{\lambda=\pm 1} u_\lambda(p)\bar{u}_\lambda(p) = \not{p} + m. \tag{5}$$

We attribute a negative mass to anti particles and use u_λ for both incoming fermions and outgoing anti fermions. We define ω_λ by

$$\omega_\lambda = (1 + \lambda\gamma^5)/2. \tag{6}$$

Now we are going to write our spinors in terms of basic ones that, if well chosen, will greatly facilitate our calculations. First we define two four-vectors k_0 and k_1 that satisfy the following conditions:

$$\begin{aligned} &k_0 \cdot k_0 = 0 \\ &k_1 \cdot k_1 = -1 \\ &k_0 \cdot k_1 = 0 \\ &k_0 \cdot p_i \neq 0 \quad \forall p_i. \end{aligned} \tag{7}$$

If the beam is directed along the z-axis a good choice for

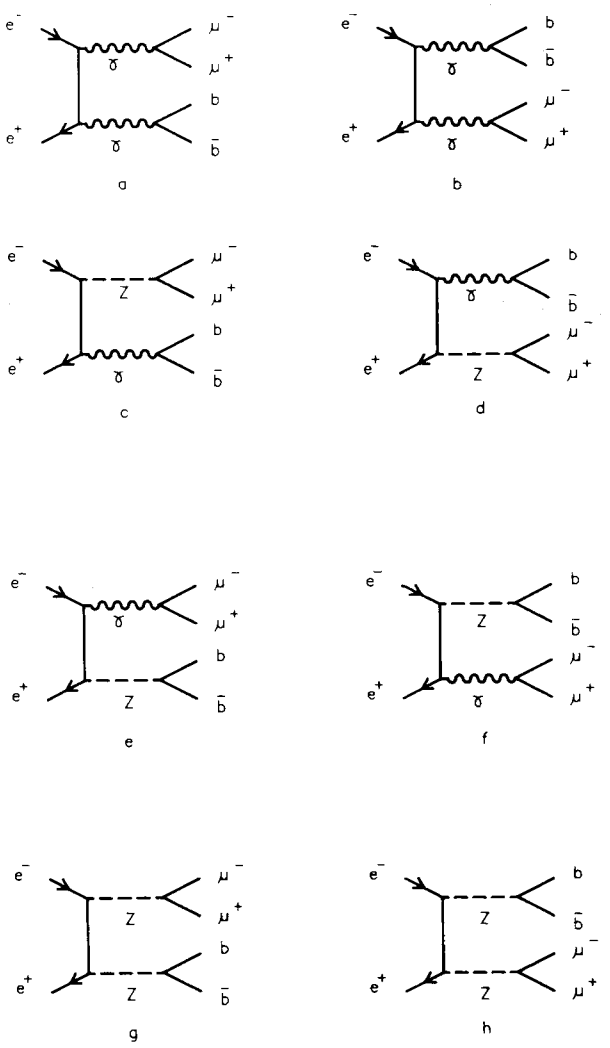

Fig. 2 a–h. Feynman diagrams for the background

k_0 and k_1 is:

$$\begin{aligned} &k_0 = (1, 1, 0, 0) \\ &k_1 = (0, 0, 0, 1). \end{aligned} \tag{8}$$

We introduce basic spinors which satisfy:

$$\begin{aligned} &u_\lambda(k_0)u_\lambda(k_0) = \omega_\lambda k_0 \\ &\quad u_+(k_0) = k_1 u_-(k_0). \end{aligned} \tag{9}$$

Where $\omega_\lambda = (1 + \lambda\gamma^5)/2$. And write the spinor $u_\lambda(p)$ in terms of the basic ones

$$u_\lambda(p_i) = (p_i + m_i)u_{-\lambda}(k_0)/\eta_i; \quad \eta_i = \sqrt{2p_i \cdot k_0}. \tag{10}$$

These spinors satisfy the Dirac-equation and their form defines a special choice for the polarization vector s:

$$s^\mu = \frac{p^\mu}{m} - \frac{m}{p \cdot k_0} k_0^\mu. \tag{11}$$

Now we introduce two scalar products of the spinors, S and T.

$$\begin{aligned} &S(p, q) := \bar{u}_+(p)u_-(q) \\ &T(p, q) := \bar{u}_-(p)u_+(q). \end{aligned} \tag{12}$$

If we write the spinors u in terms of the basic ones, using (10) we find:

$$S(p,q) = \bar{u}_-(k_0)(\not{p} + m_p)(\not{q} + m_q)\not{k}_1 u_-(k_0)/(\eta_p \eta_q)$$
$$= Tr[\omega_- \not{k}_0 \not{p} \not{q} \not{k}_1 (\eta_p \eta_q)]$$
$$= 2[p\cdot k_0 q\cdot k_1 - p\cdot k_1 q\cdot k_0 - i\varepsilon(k_0, k_1, p, q)]/(\eta_p \eta_q). \quad (13)$$

With $\varepsilon(k_0, k_1, p, q)$ the Levi–Civita tensor fully contracted with k_0, k_1, p and q. Substituting (8) in (13) leads to:

$$S(p,q) = (p_y + ip_z)\frac{\eta_q}{\eta_p} - (q_y + iq_z)\frac{\eta_p}{\eta_q}$$
$$T(p,q) = S(q,p)^*. \quad (14)$$

The next step is to split up the spinor $u_\lambda(p)$ in two parts:

$$u_\lambda(p) = \alpha_\lambda(p) + \mu u_{-\lambda}(k_0). \quad (15)$$

With $\mu = m/\eta$ and $\alpha_\lambda(p) = \not{p} u_\lambda(k_0)/\eta$. The following relations are easily verified:

$$S(p,q) = \bar{\alpha}_+(p)\alpha_-(q); \quad T(p,q) = \bar{\alpha}_-(p)\alpha_+(q). \quad (16)$$

As this point we introduce the Z and Y functions. The Z function represents a four fermion process with an intermediate photon or Z. It is defined as:

Table 1. The Z-functions

$Z(+,+,+,+)$	$-2(h_a h_b s_{13} t_{24} - g_a h_b \mu_1 \mu_2 \eta_3 \eta_4 - h_a g_b \eta_1 \eta_2 \mu_3 \mu_4)$
$Z(+,+,+,-)$	$-2\eta_2(h_a h_b \mu_4 s_{13} - h_a g_b \mu_3 s_{14})$
$Z(+,+,-,+)$	$-2\eta_1(h_a g_b \mu_4 t_{23} - h_a h_b \mu_3 t_{24})$
$Z(+,+,-,-)$	$-2(h_a g_b s_{14} t_{23} - g_a g_b \mu_1 \mu_2 \eta_3 \eta_4 - h_a h_b \eta_1 \eta_2 \mu_3 \mu_4)$
$Z(+,-,+,+)$	$-2\eta_4(h_a h_b \mu_2 s_{31} - g_a h_b \mu_1 s_{32})$
$Z(+,-,+,-)$	0
$Z(+,-,-,+)$	$2(g_a h_b \mu_1 \mu_3 \eta_2 \eta_4 - g_a g_b \mu_1 \mu_4 \eta_2 \eta_3$ $- h_a h_b \mu_2 \mu_3 \eta_1 \eta_4 + h_a g_b \mu_2 \mu_4 \eta_1 \eta_3)$
$Z(+,-,-,-)$	$-2\eta_3(h_a g_b \mu_2 s_{41} - g_a g_b \mu_1 s_{42})$
$Z(-,+,+,+)$	$-2\eta_3(g_a h_b \mu_2 t_{41} - h_a h_b \mu_1 t_{42})$
$Z(-,+,+,-)$	$2(h_a g_b \mu_1 \mu_3 \eta_2 \eta_4 - h_a h_b \mu_1 \mu_4 \eta_2 \eta_3$ $- g_a g_b \mu_2 \mu_3 \eta_1 \eta_4 + g_a h_b \mu_2 \mu_4 \eta_1 \eta_3)$
$Z(-,+,-,+)$	0
$Z(-,+,-,-)$	$-2\eta_4(g_a g_b \mu_2 t_{31} - h_a g_b \mu_1 t_{32})$
$Z(-,-,+,+)$	$-2(g_a h_b t_{14} s_{23} - h_a h_b \mu_1 \mu_2 \eta_3 \eta_4 - g_a g_b \eta_1 \eta_2 \mu_3 \mu_4)$
$Z(-,-,+,-)$	$-2\eta_1(g_a h_b \mu_4 s_{23} - g_a g_b \mu_3 s_{24})$
$Z(-,-,-,+)$	$-2\eta_2(g_a g_b \mu_4 t_{13} - g_a h_b \mu_3 t_{14})$
$Z(-,-,-,-)$	$-2(g_a g_b t_{13} s_{24} - h_a g_b \mu_1 \mu_2 \eta_3 \eta_4 - g_a h_b \eta_1 \eta_2 \mu_3 \mu_4)$

$$Z(p_1, \lambda_1, p_2, p_3, \lambda_3, p_4, \lambda_4, g_a, h_a, g_b, h_b)$$
$$= \bar{u}_{\lambda_1}(p_1)\gamma^\mu(g_a\omega_- + h_a\omega_+)u_{\lambda_2}(p_2)\bar{u}_{\lambda_3}(p_3)$$
$$\cdot\gamma_\mu(g_b\omega_- + h_b\omega_+)u_{\lambda_4}(p_4) \quad (17)$$

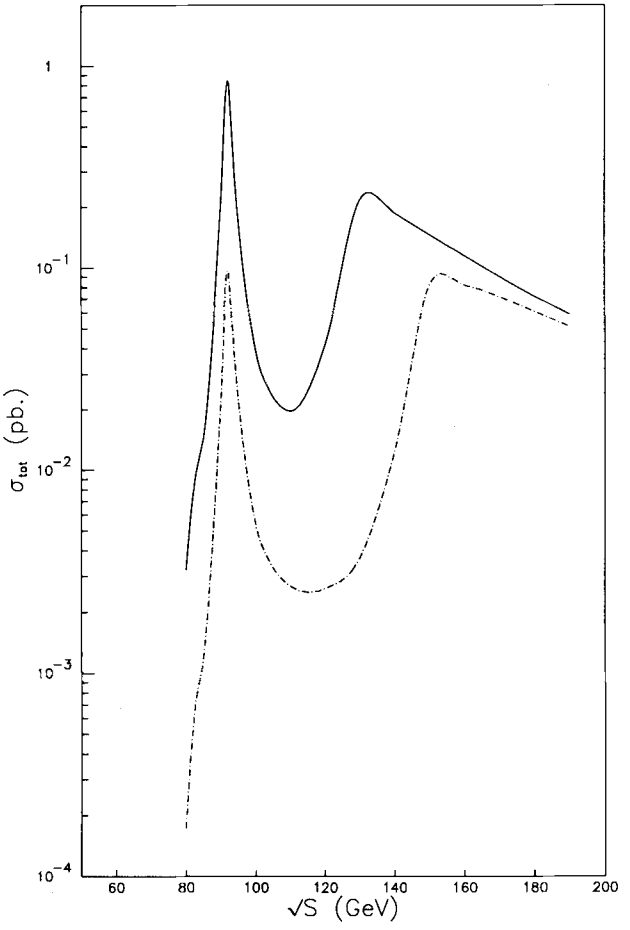

Fig. 3. Total cross section as function of the c.m.s. energy for process 1 only. $M_H = 30$ (solid line) and $M_H = 50$ (dashed line)

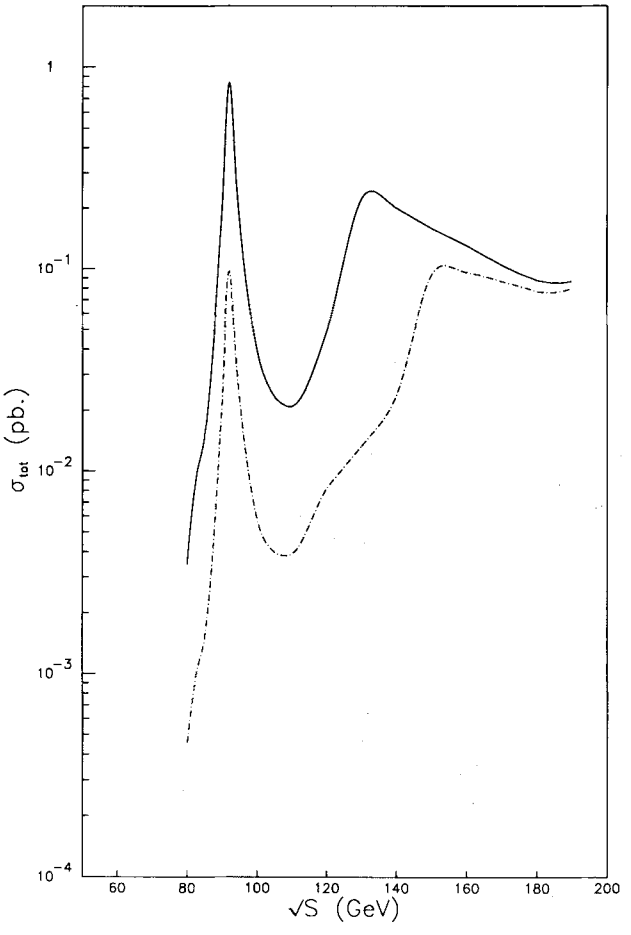

Fig. 4. Total cross section as function of the c.m.s. energy for all processes

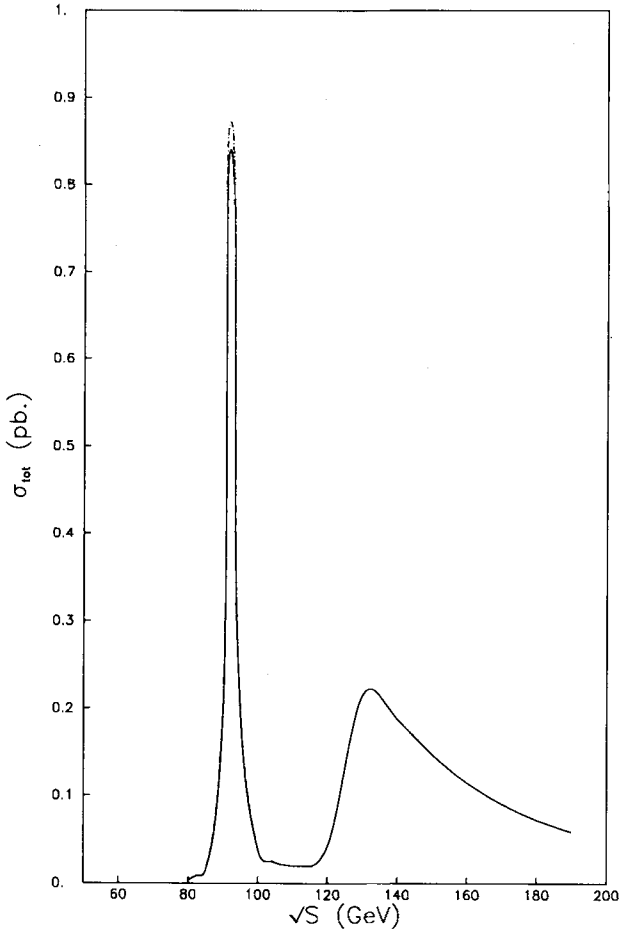

Fig. 5. Total cross section for a Higgs mass of 30 GeV, with (solid line) and without (dashed line) a cut of 20 GeV on the invariant muon pair mass

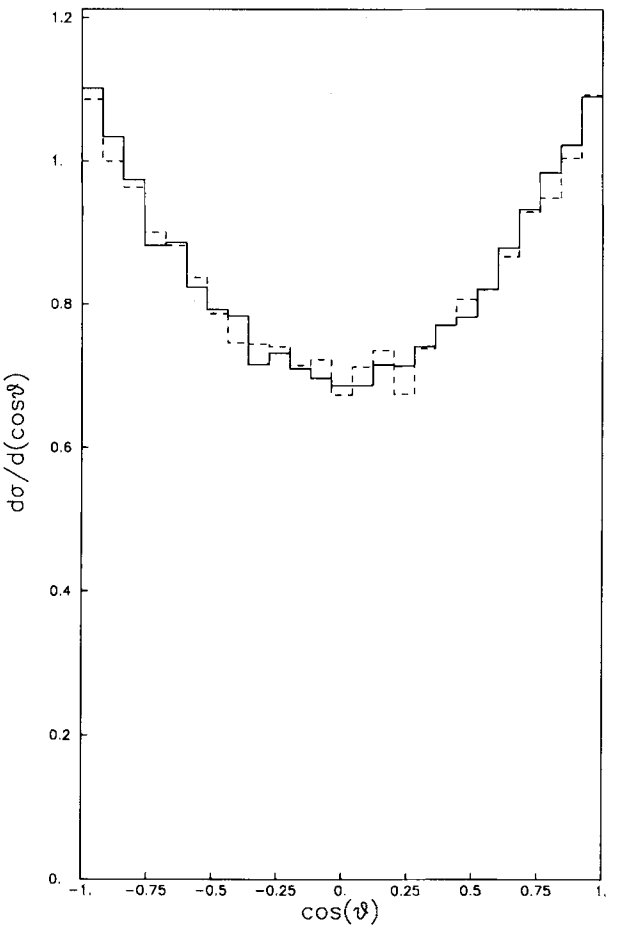

Fig. 6. Angular distributions of the muons, $M_H = 30$ GeV, $\sqrt{S} = 92$ GeV, Higgs only = solid line, Higgs + background = dashed line

with $p_1 \cdots p_4$ the four momenta of the participating particles and $\lambda_1 \cdots \lambda_4$ their spin. The term $(g\omega_- + h\omega_+)$ is the left-right coupling of the fermion pair. In case of an intermediate photon we have $g = h = 1$ and this factor vanishes. For each polarisation configuration it is possible to express Z in terms of the S and T functions and the coupling constants. The calculation is done in detail in [1]. We give the results in Table 1.

The Y function represents the decay of a scalar particle into a fermion pair. It is defined as:

$$Y(\lambda_1, \lambda_2) = Y(p_1, \lambda_1, p_2, \lambda_2) := \bar{u}_{\lambda_1}(p_1) u_{\lambda_2}(p_2). \tag{18}$$

Its calculation is relatively easy:

$$\begin{aligned} Y(+,+) &= \bar{u}_+(p_1) u_+(p_2) \\ &= \bar{u}_+(k_0)(\not{p}_1 + m1)(\not{p}_2 + m2) u_+(k_0)/\eta_1\eta_2 \\ &= \mathrm{Tr}[\omega_- \not{k}_0(\not{p}_1 + m1)(\not{p}_2 + m2)]/\eta_1\eta_2 \\ &= \mu_2/\eta_1 \,\mathrm{Tr}[\omega_- \not{k}_0 \not{p}_1] + \mu_1/\eta_2 \,\mathrm{Tr}[\omega_- \not{k}_0 \not{p}_2] \\ &= \mu_2/\eta_1 (2k_0 \cdot p_1) + \mu_1/\eta_2 (2k_0 \cdot p_2) \\ &= \mu_2\eta_1 + \mu_1\eta_2. \end{aligned} \tag{19}$$

And in a similar way we find:

$$\begin{aligned} Y(+,-) &= S(p_1, p_2) \\ Y(-,+) &= T(p_1, p_2) \\ Y(-,-) &= \mu_2\eta_1 + \mu_1\eta_2. \end{aligned}$$

We still have to demonstrate that the amplitude for the processes of diag. 1 and 2 can be written in terms of Y and Z functions. Before we do so we note that if the Z couples to very light fermions, as is the case in diag. 1 and 2, we can neglect the $k^\mu k^\nu / M_Z^2$ in the Z propagator and write it as $-ig^{\mu\nu}/(k^2 - M_Z^2)$. In this case we can write the amplitude $\mathcal{M}$ for diagram 1 as:

$$\mathcal{M} = \frac{8ie_4}{\sin^4 2\theta_w [(p_1+p_2)^2 - M_Z^2][(p_3+p_4)^2 - M_Z^2][(p_5+p_6)^2 - m_H^2]} \frac{m_b}{\bar{u}_{\lambda_2}(p_2)\gamma^\mu(g^e\omega_- + h^e\omega_+)u_{\lambda_1}(p_1)\bar{u}_{\lambda_3}(p_3)\gamma_\mu (g^\mu\omega_- + h^\mu\omega_+)u_{\lambda_4}(p_4)\bar{u}_{\lambda_5}(p_5)u_{\lambda_6}(p_6)} \tag{20}$$

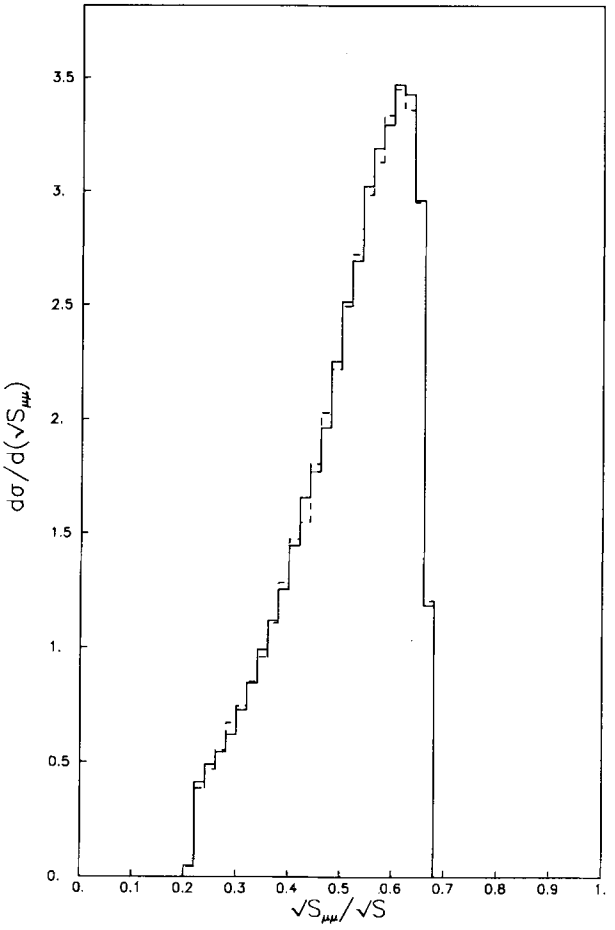

Fig. 7. Invariant mass of the muon pair, $M_H = 30\,\text{GeV}$, $\sqrt{S} = 92\,\text{GeV}$

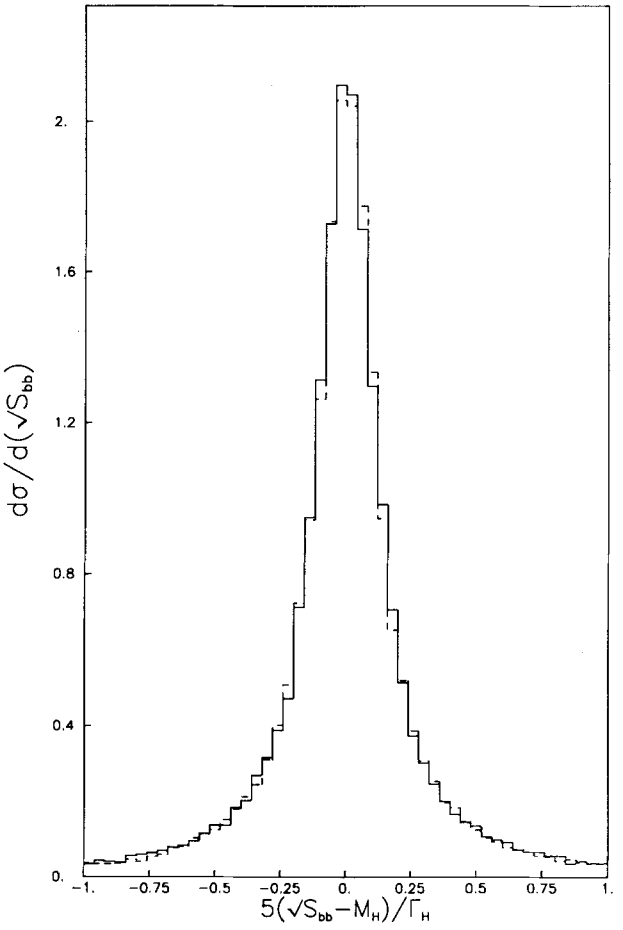

Fig. 8. Blow-up picture of the Higgs peak, $M_H = 30\,\text{GeV}$, $\sqrt{S} = 92\,\text{GeV}$

with θ_W the Weinberg angle. With the definitions of the Z and Y functions this becomes:

$$\mathcal{M} = C \cdot Z(p_1, \lambda_1, \ldots, p_4, \lambda_4) \cdot Y(p_5, \lambda_5, p_6, \lambda_6). \tag{21}$$

For the processes of Fig. 2 the matrix element is more complicated. As an example we treat the diagram of Fig. 2f. The matrix element is given by:

$$\mathcal{M} = \frac{-i4e^4}{\sin^2 2\theta_w} \cdot \frac{\mathcal{A}(p_1, \lambda_1, p_2, \lambda_2, p_3, \lambda_3, p_4, \lambda_4, p_5, \lambda_5, p_6, \lambda_6)}{(p_3+p_4)^2[(p_1-p_5-p_6)^2-m_1^2][(p_5+p_6)^2-M_Z^2]}. \tag{22}$$

The spinorial part of $\mathcal{M}$ is contained in $\mathcal{A}$:

$$\begin{aligned}\mathcal{A}&(p_1, \lambda_1, \ldots, p_6, \lambda_6) \\ &= \bar{u}_{\lambda_2}(p_2)\gamma_\nu[(\not{p}_1 + m_1) - (\not{p}_5 + m_5) - (\not{p}_6 + m_6)] \\ &\quad \cdot \gamma_\mu u_{\lambda_1}(p_1)\bar{u}_{\lambda_5}(p_5)\gamma^\mu(g_\mu\omega_- + h_\mu\omega_+) \\ &\quad \cdot u_{\lambda_6}(p_6)\bar{u}_{\lambda_3}(p_3)\gamma^\mu u_{\lambda_4}(p_4).\end{aligned} \tag{23}$$

Now using the definition of the Z-function and the normalisation condition (9) we can write:

$$\begin{aligned}\mathcal{A}&(p_1, \lambda_1, p_2, \ldots, p_6, \lambda_6) \\ &= \sum_{\lambda = \pm 1} \{Z(p_2, \lambda_2, p_1, \lambda, p_3, \lambda_3, p_4, \lambda_4) \\ &\quad \cdot Z'(p_1, \lambda, p_1, \lambda_1, p_5, \lambda_5, p_6, \lambda_6) \\ &\quad - Z(p_2, \lambda_2, p_5, \lambda, p_3, \lambda_3, p_4, \lambda_4) \\ &\quad \cdot Z'(p_5, \lambda, p_1, \lambda_1, p_5, \lambda_5, p_6, \lambda_6) \\ &\quad - Z(p_2, \lambda_2, p_6, \lambda, p_3, \lambda_3, p_4, \lambda_4) \\ &\quad \cdot Z'(p_6, \lambda, p_1, \lambda_1, p_5, \lambda_5, p_6, \lambda_6)\}\end{aligned} \tag{24}$$

where Z denotes a Z function with an intermediate photon, and Z' a Z function with an intermediate Z boson. This means that once we have calculated the Z and Y functions we only need to fill in (20) and (22) to find the amplitude. We proceed as follows.

- Calculate S and T for all combinations.
- Calculate the Z and Y functions for a given polarisation configuration.
- Sum the contribution of all diagrams.
- Square this sum over all polarisation states.

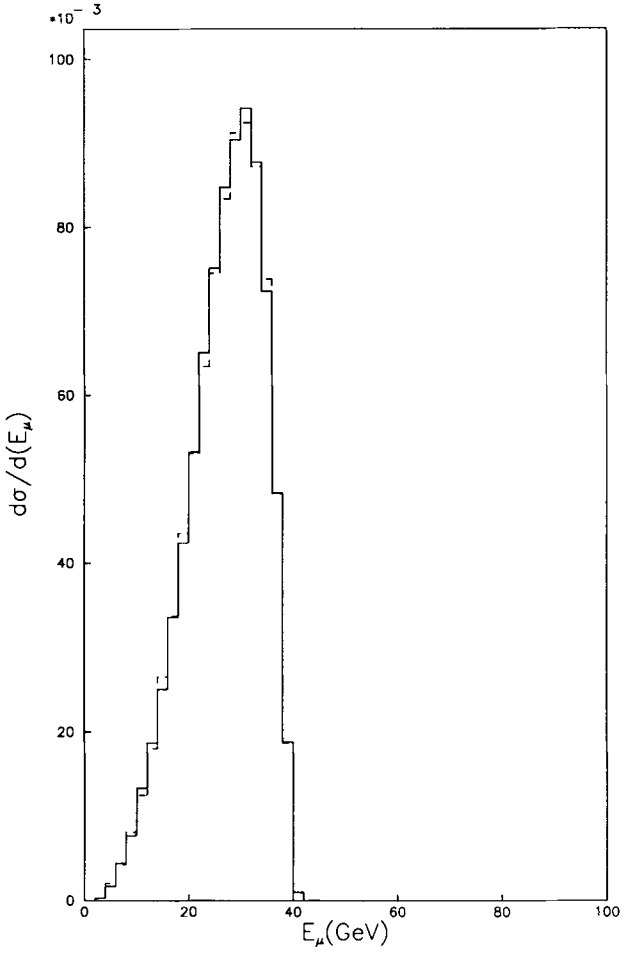

Fig. 9. Energy distribution of the muons, $M_H = 30\,\text{GeV}$, $\sqrt{S} = 92\,\text{GeV}$

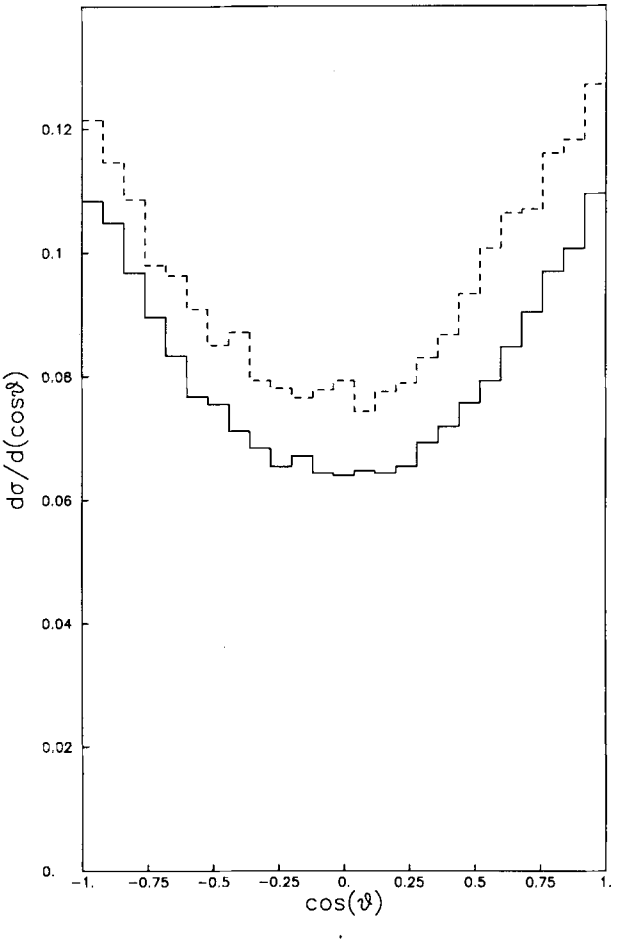

Fig. 10. Angular distributions of the muons, $M_H = 50\,\text{GeV}$, $\sqrt{S} = 162\,\text{GeV}$, Higgs only = solid line, Higgs + background = dashed line

We have done this numerically. The results can be found in Sect. 4.

3 Kinematics

In order to define the kinematics we introduce the four momenta of the initial and final state particles as follows:

$$e^-(p_1) + e^+(p_2) \to \mu^-(p_3) + \mu^+(p_4) + b(p_5) + \bar{b}(p_6). \quad (25)$$

We also introduce the auxilary variables $q_{12} = p_1 + p_2$, $q_{34} = p_3 + p_4$ and $q_{56} = p_5 + p_6$. It is to be noticed that q_{12} is the total c.m.s. four momentum, q_{34} is the four momentum running through the final Z propagator in Fig. 1 and likewise q_{56} is the four momentum through the Higgs propagator. In terms of these variables we can write the four particle phase space as:

$$dR^4 = (2\pi)^4 \delta^4(p_3 + p_4 + p_5 + p_6 - p_1 - p_2) d\omega(\mathbf{p}_3) \cdots d\omega(\mathbf{p}_6) \quad (26)$$

where we have introduced the notation

$$d\omega(\mathbf{p}) = \frac{d^3p}{(2\pi)^3 2p_0}; \quad p_0 = \sqrt{\mathbf{p}^2 + m^2} \quad (27)$$

we can rewrite the phase space element as:

$$dR^4 = (2\pi)^4 \delta^4(q_{34} + q_{56} - p_1 - p_2) d\omega(\mathbf{q}_{34}) d\omega(\mathbf{q}_{56}) \cdot (2\pi)^4 \delta^4(p_3 + p_4 - q_{34}) d\omega(\mathbf{p}_3) d\omega(\mathbf{p}_4) \frac{ds_{34}}{2\pi} \cdot (2\pi)^4 \delta^4(p_5 + p_6 - q_{56}) d\omega(\mathbf{p}_5) d\omega(\mathbf{p}_6) \frac{ds_{56}}{2\pi}. \quad (28)$$

Here we have introduced the invariant mass variables

$$s_{34} = q_{34}^2; \quad s_{56} = q_{56}^2. \quad (29)$$

From expression (3.4) we see that the phase space integral factorizes into a quasi two body to two body process, followed in each case by a two body decay. If we now consider the diagram of Fig. 1 only we see that the amplitude contains among other things the Higgs propagator

$$\frac{1}{s_{56} - M_H^2 + iM_H\Gamma_H} \quad (30)$$

as a factor. In the differential cross section this gives rise

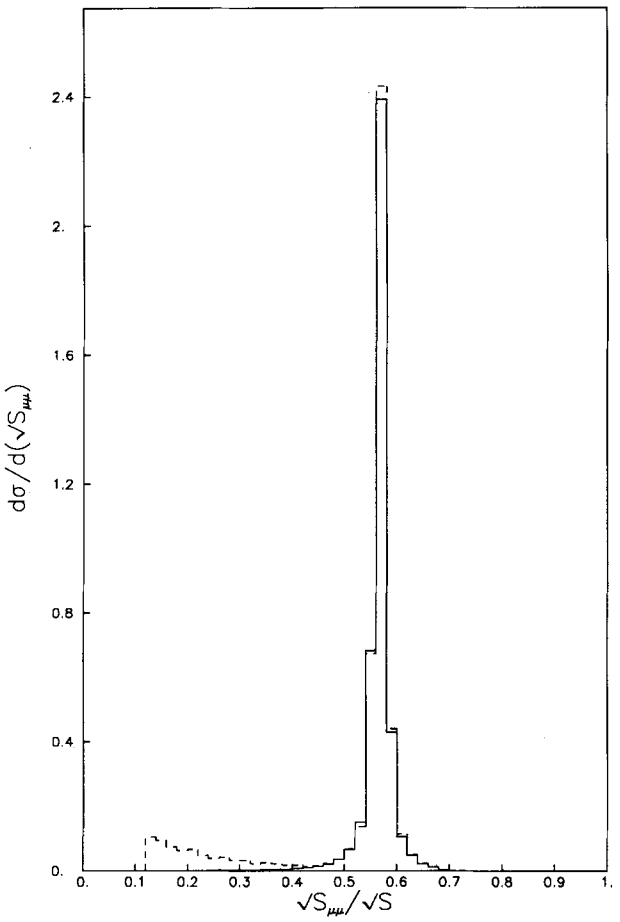

Fig. 11. Invariant mass of the muon pair, $M_H = 50\,\text{GeV}$, $\sqrt{S} = 162\,\text{GeV}$

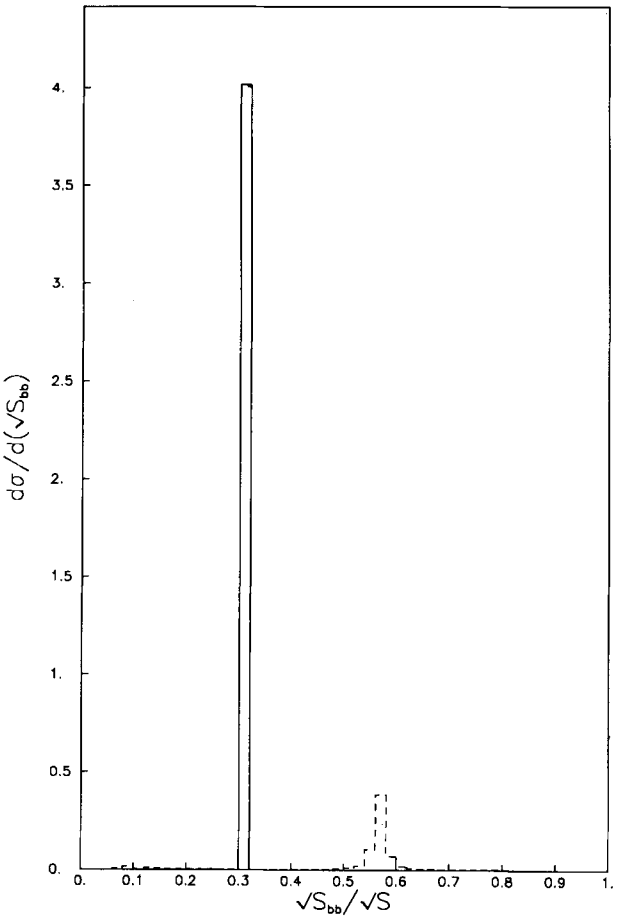

Fig. 12. Invariant mass of the b pair, $M_H = 50\,\text{GeV}$, $\sqrt{S} = 162\,\text{GeV}$

to a factor

$$\frac{1}{(s_{56} - M_H^2)^2 + M_H^2 \Gamma_H^2}. \tag{31}$$

We can see now that the integration over s_{56} has the following form:

$$\int \frac{1}{(s_{56} - M_H^2)^2 + M_H^2 \Gamma_H^2} f(s_{56}) \frac{ds_{56}}{2\pi} \tag{32}$$

where $f(s_{56})$ is a smoothly varying function around M_H. Since the Higgs is relatively narrow i.e. $\Gamma_H \ll M_H$, this integral has a sharply peaked integrand. In order to get a stable Monte Carlo integration we transform to a new variable σ_{56} by means of the following expression.

$$s_{56} = M_H^2 + M_H \Gamma_H \tan \sigma_{56}. \tag{33}$$

The integral can now be written as:

$$\frac{1}{2\pi M_H \Gamma_H} \int f(M_H^2 + M_H \Gamma_H \tan \sigma_{56}) d\sigma_{56} \tag{34}$$

a form which is more suitable for numerical integration. We should mention here that also in the case where the diagrams of Fig. 2 contribute we use this transformation of variables.

Another problem occurs if we allow for very small invariant masses of the μ pair. This is caused by the sharp peaking of the photon propagators in Fig. 2a-b. We circumvent this problem by imposing a lower limit on the μ pair invariant mass of 20 GeV. We have convinced ourselves that this cut does not reduce the Higgs signal appreciably. We come back to this point in Sect. 4. Apart from these points the integration over phase space by means of a Monte Carlo routine (we have used the program VEGAS [7]) is straightforward.

4 Results and conclusions

In this section we will present results on Higgs production and background for LEP energies. For definiteness we start with a few numerical constants which we used in the calculation. The mass of the b quark we take to be 5 GeV. For the Z mass we take 92 GeV. Using the particle data table values for G_f and α this leads to the (tree level) value of the weak mixing angle of $\sin^2 \theta_w = 0.207$. In all our calculations we consider values for M_H in the range 10–80 GeV. For the coupling of the Higgs to fermions we take the value $G_f \sqrt{2} m_f$. One important quantity is the branching ratio $B(H \to b\bar{b})$. In order to calculate this (at tree level) we need the masses of all quarks and leptons.

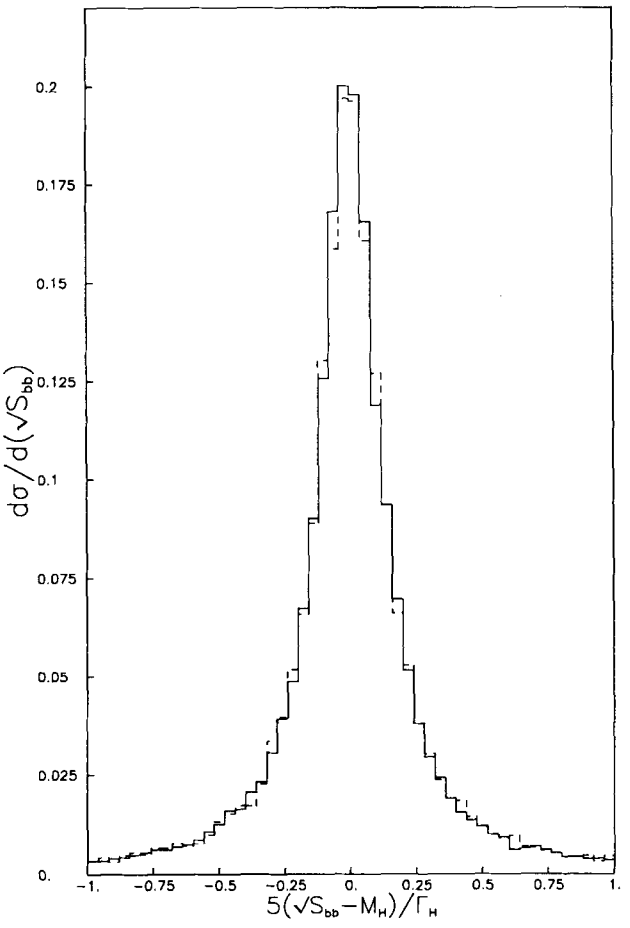

Fig. 13. Blow-up picture of the Higgs peak, $M_H = 50\,\text{GeV}$, $\sqrt{S} = 162\,\text{GeV}$

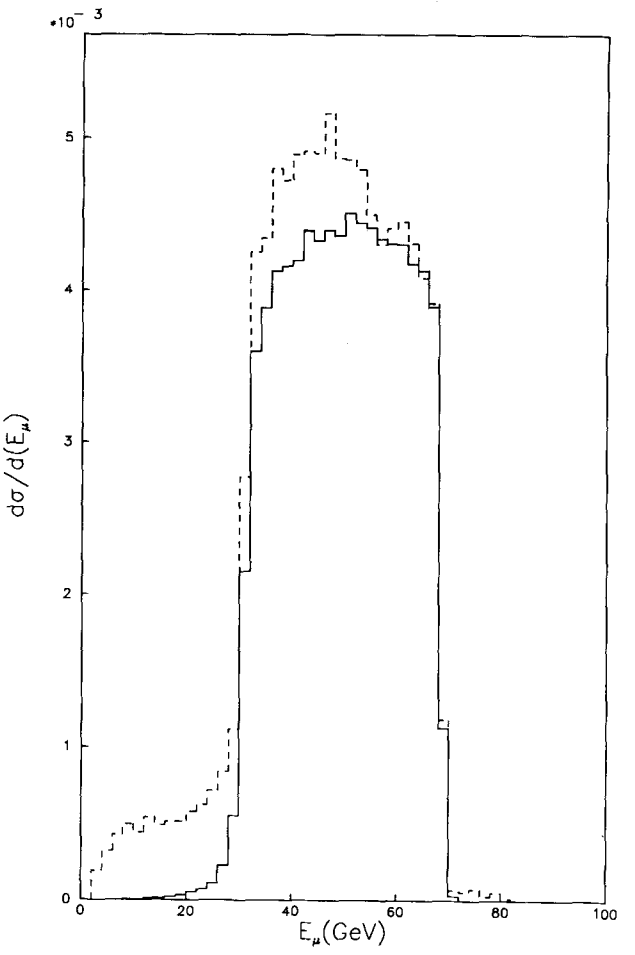

Fig. 14. Energy distribution of the muons, $M_H = 50\,\text{GeV}$, $\sqrt{S} = 162\,\text{GeV}$

For the leptons we take the standard model values, for u and d we take 0.1 GeV, for s we take 0.5 GeV and for c 1.5 GeV. In Table 1 we give the branching ratios and the total width as a function of the Higgs mass.

For reference purposes we give in Fig. 3 the total cross section for process (4) for a Higgs mass of 30 and 50 GeV where we only take into account diag. 1. It is to be noted here that this is a very good approximation to $\sigma(e^+e^- \to \mu^+\mu^- H) \cdot B(H \to b\bar{b})$ except for the fact that all effects due to a finite Higgs width have now been taken into account.

Table 2. The total width and the branching ratios of the Higgs for various masses

M_H(GeV)	$\Gamma(H)$(GeV)	$B(H \to \tau\bar{\tau})$	$B(H \to c\bar{c})$	$B(H \to b\bar{b})$
5	$0.150\,10^{-4}$	0.240	0.758	0.000
8	$0.403\,10^{-4}$	0.298	0.701	0.000
10	$0.556\,10^{-4}$	0.307	0.692	0.000
12	$0.170\,10^{-3}$	0.128	0.284	0.587
15	$0.397\,10^{-3}$	0.072	0.157	0.770
20	$0.765\,10^{-3}$	0.052	0.112	0.836
25	$0.111\,10^{-2}$	0.046	0.098	0.856
30	$0.143\,10^{-2}$	0.043	0.092	0.865
40	$0.205\,10^{-2}$	0.040	0.086	0.874
50	$0.264\,10^{-2}$	0.039	0.083	0.877
60	$0.322\,10^{-2}$	0.039	0.082	0.879

In Fig. 4 we consider the total cross section taking into account all diagrams from Figs. 1 and 2. Here we impose a cut on the μ pair invariant mass $s_{34} > (20\,\text{GeV})^2$. It is clear that for this case we have the Higgs production diagram, the background and the interference. In Fig. 5 we again plot the total cross section for a Higgs mass of 30 GeV as a function of $\sqrt{s}$, with and without this cut. It shows that the cut does not affect the Higgs signal significantly.

In Fig. 6–9 we look at some distributions at the Z peak for a Higgs mass of 30 GeV with and without background. Figure 6 shows the angular distribution of the muons, respective to the Z-axis. In Fig. 7 we look at the distribution of the invariant mass of the μ-pair. Figure 8 is a blow up picture of the invariant mass distribution of the $b\bar{b}$-pair, centered around the Higgs mass. The energy distribution of the muons is shown in Fig. 9. From the figures it is obvious that the background processes are negligible compared to Higgs production.

A different picture we get when we look at Figs. 10–14. Here we have plotted the same distribution, with and without background, but this time for a Higgs mass of 50 GeV and a $\sqrt{s} = 162\,\text{GeV}$. We see that the total cross

section for Higgs production and background is enlarged by 15% with respect to the cross section for Higgs production only. The shape of the angular distribution does not change much, but the invariant mass distributions do. For the invariant μ-pair mass distribution (Fig. 11) we see a tail at low masses, coming from the processes of Fig. 2e and 2f, and a smaller effect at the Z mass, coming from the double Z diagrams. In the invariant $b\bar{b}$ mass distribution (Fig. 12) we see a second peak at much higher masses, coming from a real Z decaying into a b pair. The blow up picture of the Higgs peak shows no evidence for Higgs-background interference. The muon energy distribution (Fig. 14) for the background has a rather flat shape and goes up till the same values as for the Higgs production process.

From the result we conclude that for LEP 1 energies the background coming from two photon/Z processes can be eliminated with a simple cut on the invariant muon pair mass. For a Higgs of 50 GeV or more we shall have to go to LEP 200 energies. For c.m.s. energies of 120 GeV and higher we find a sizable effect of the background and will need more sophisticated cuts. This will be even more true in the case that we don't have b identification and the background will be four times as big and of the same order as the signal. In addition to that, as we go to higher energies, to find a Higgs heavier than 50 GeV the contribution of the $2Z$ diagrams becomes more important. A possible way to reduce the background is to raise the cut on the invariant μ-pair mass. As long as $M_Z + M_H \leqq E^{\text{c.m.s.}}$ the μ-pair in Higgs production will have a mass close to the Z mass. Putting the cut at 60 GeV in Fig. 11 would cut away most of the μ-pairs coming from a photon or an off-shell Z. Another useful quantity to reduce the background is the invariant $b\bar{b}$ mass. By cutting away masses above 80–85 GeV. We eliminate most of the double Z background (see Fig. 12). This only works if the mass of the Higgs is below 80 GeV. A cut on the energy of the muons is also possible, but less effective than the invariant mass cut.

References

1. R.N. Cahn: Rep. Prog. Phys. 52 (1989) 389
2. Sau Lan Wu et al., in: ECFA workshop on LEP 200, CERN 87-08 (1987) Vol. 2
3. P.J. Franzini, P. Taxil, in: Z Physics at LEP 1, CERN 89-08 (1989) Vol. 2
4. F.A. Berends, R. Kleiss: Nucl. Phys. B260 (1985) 32
5. ALEPH Coll.: Phys. Lett. 236B (1990) 233
6. F.A. Berends, P.H. Daverveld, R. Kleiss: Nucl. Phys. B253 (1985) 441.
7. G.P. Lepage VEGAS Coll.: J. Comp. Phys. 27 (1978) 192